Evolution, 2025, **79(7)**, 1185–1198
https://doi.org/10.1093/evolut/qpaf047
Advance access publication 20 May 2025
Original Article

Effect of assortative mating and sexual selection on polygenic barriers to gene flow

Parvathy Surendranadh[1] **and Himani Sachdeva**[2]

[1]Institute of Science and Technology Austria, Klosterneuburg, Austria
[2]Department of Mathematics, University of Vienna, Vienna, Austria

*Corresponding author: Institute of Science and Technology Austria, Am Campus 1, 3400 Klosterneuburg, Austria. Email: parvathy.surendranadh@ist.ac.at

Abstract

Assortative mating and sexual selection are widespread in nature and can play an important role in speciation by facilitating the buildup and maintenance of reproductive isolation (RI). However, their contribution to genome-wide suppression of gene flow during RI is rarely quantified. Here, we consider a polygenic "magic" trait that is divergently selected across two populations connected by migration, while also serving as the basis of assortative mating, thus generating sexual selection on one or both sexes. We obtain theoretical predictions for divergence at individual trait loci by assuming that the effect of all other loci on any locus can be encapsulated via an effective migration rate, which bears a simple relationship to measurable fitness components of migrants and various early-generation hybrids. Our analysis clarifies how "tipping points" (characterized by an abrupt collapse of adaptive divergence) arise, and when assortative mating can shift the critical level of migration beyond which divergence collapses. We quantify the relative contributions of viability and sexual selection to genome-wide barriers to gene flow and discuss how these depend on existing divergence levels. Our results suggest that effective migration rates provide a useful way of understanding genomic divergence, even in scenarios involving multiple, interacting mechanisms of RI.

Keywords: assortative mating, sexual selection, effective migration rates, polygenic selection, reproductive isolation

Introduction

Reproductive isolation (RI) typically results from the interaction of multiple processes that cause loss of hybrid fitness, thus reducing gene flow between populations. Ecological specialization arising from adaptation to different environmental niches, immigrant inviability, or intrinsic genetic incompatibilities may all generate postzygotic barriers to gene flow and maintain genetic differences between populations (Coughlan and Matute, 2020; Rice and Hostert, 1993; Rundle and Nosil, 2005). Additionally, processes such as assortative mating and sexual selection can act as both prezygotic and postzygotic barriers—by reducing heterospecific matings (that produce hybrids) as well as the mating success of hybrids. Indeed, it has been argued that the buildup of RI typically involves coupling between both postzygotic and prezygotic barriers (Butlin and Smadja (2018)).

Assortative mating (AM)—which involves positive phenotypic (and genetic) correlation between mating pairs (Lewontin et al. (1968)), is especially common in animals Jiang et al. (2013). Numerous studies have documented its role during RI, for example, in cichlids (Elmer et al., 2009; Stelkens and Seehausen, 2009), swordtail fish (Schumer et al., 2017), sticklebacks (Vines and Schluter, 2006), butterflies (Jiggins et al., 2001), and marine snails (Johannesson et al., 2008). AM decreases heterozygosity and genic variance within a population but simultaneously increases total genetic variance (by generating higher levels of linkage disequilibria [LD]) (Lynch et al., 1998), thus increasing the potential for divergence and speciation.

AM may occur either due to temporal or spatial separation of population groups, via preference-trait mechanisms, or via phenotype matching between potential mates (Jiang et al., 2013; Kirkpatrick and Ravigné, 2002; Kopp et al., 2018). Each mechanism differs in the extent of sexual selection it generates—ranging from strong sexual selection under phenotype matching to almost none when assortment is due to temporal or spatial separation. Sexual selection typically reduces the mating success of rare phenotypes and thus may counteract the effects of AM (Safran et al. (2013); Servedio and Boughman (2017)). For example, when AM involves sexual selection on both sexes (e.g., if both males and females suffer reduced mating opportunities by being choosy), then its net effect is to generate stabilizing selection and inhibit divergence (Kirkpatrick and Nuismer (2004)).

Numerous studies have examined how different isolating mechanisms, namely assortative mating (Doebeli, 1996; Kondrashov and Shpak, 1998; Kopp et al., 2018), ecological selection (Smith, 1966; Maan and Seehausen, 2011), and sexual selection (Schumer et al., 2017; Servedio, 2016; Servedio and Kopp, 2012), influence divergence and RI in the presence of ongoing gene flow. These suggest that RI is facilitated by coupling between traits that act as reproductive barriers

Received July 31, 2024; revisions received January 02, 2025; accepted March 06, 2025
Associate Editor: Jonathan Henshaw; Handling Editor: Tim Connallon

(Kirkpatrick and Ravigné, 2002; Coyne and Allen Orr, 2004; Smadja and Butlin, 2011). Such coupling can arise when loci underlying different traits are tightly linked and not easily broken apart by recombination, or if loci have pleiotropic effects on multiple traits (Butlin and Smadja, 2018; Felsenstein, 1981; Servedio, 2009; Smadja and Butlin, 2011). In this regard, speciation is thought to be most effective with magic traits, that is, if the same trait is under divergent selection and also mediates AM. Magic traits are now known to be more common than previously assumed (Servedio et al. (2011a)): well-known examples include wing color pattern in Heliconius (Merrill et al. (2012)) and body size in Littorina (Perini et al. (2020)).

Magic traits may differ in their mechanism of AM and the extent to which they are under sexual selection, and have been studied extensively to understand the evolution of mate choice during speciation (Servedio and Boughman, 2017; Servedio and Kopp, 2012; Servedio et al., 2011b). While previous work has mostly focused on few-locus models of mate choice, here we consider a polygenic trait influenced by many small-effect alleles. Not only is this more realistic in view of the polygenic architecture of most traits but also much less understood, with previous studies relying largely on simulation of two populations (Sachdeva and Barton, 2017; Muralidhar et al., 2022) or of hybrid zones (Irwin, 2020; Perini et al., 2020). In general, the evolution of polygenic divergence and RI depends on the ease with which *multiple* locally advantageous alleles can establish and/or be maintained across the genome despite maladaptive gene flow between populations. This in turn depends on whether selected loci evolve more or less independently, or whether LD between sets of maladapted alleles causes them to be eliminated *together* before they can recombine onto fitter backgrounds. This was first studied in the context of hybrid zones, where it was found that the strength of LD between multiple selected loci depends on the ratio of total selection to total recombination (Barton, 1983).

As we demonstrate here, a powerful way of analyzing the effects of LD on divergence is by tracking how introgressing alleles at any one trait locus are transferred between genetic backgrounds, typically via multiple recombination events over multiple generations. The different genetic backgrounds on which the focal allele finds itself may differ in their hybrid index (i.e., the proportion of genetic material they derive from either parental population) and thus also have different fitness values, which influences the transmission probability of the allele. This is captured by the notion of the *effective* migration rate (m_e), which is the rate at which neutral introgressing alleles are transferred between hybridising populations (Bengtsson, 1985). In essence, strong LD between large numbers of loci reduces m_e across the genome (Barton and Bengtsson, 1986). This increases divergence between hybridising populations, which reduces hybrid fitness, further decreasing effective migration rates. Indeed, it has been argued that this genome-wide reduction in m_e between hybridizing populations provides a natural way of quantifying RI (Westram et al., 2022). Subsequent work has generalized theory based on m_e to weakly selected loci with partial and/or transient divergence between populations (Sachdeva, 2022), heterogeneous effect sizes and dominance (Zwaenepoel et al., 2024), and sex-linkage (Fraïsse and Sachdeva, 2021). However, all of this work is restricted to randomly mating populations.

In this paper, we extend theory based on effective migration rates to a scenario with assortative mating due to female preference for phenotypically similar males, which leads to sexual selection on one or both sexes. The phenotype underlying assortment is polygenic and under divergent selection between a mainland and island: thus, we have a simple "magic trait" scenario of speciation. We derive expressions for m_e at an unlinked locus and then use this to predict allele frequency divergence at individual trait loci under migration-selection-assortment balance by assuming that the effect of all other loci on the focal locus is encapsulated by this effective migration rate. This allows us to predict mean trait divergence between mainland and island and explore how assortment, viability, and sexual selection jointly influence the critical threshold at which migration swamps adaptive divergence. We then use this to disentangle the relative contributions of viability and sexual selection to the genome-wide barrier to gene flow in parameter regimes where partial RI persists despite migration.

Methods

Model

Consider an island subject to one-way migration from a large mainland, such that a fraction m of individuals on the island are replaced by migrants in each generation. Individuals are haploid and hermaphroditic (i.e., produce both male and female gametes) and can thus play the male or female role during reproduction. Each individual expresses an additive polygenic trait $z = \sum_{j=1}^{L} \alpha_j X_j$ influenced by a large number L of unlinked, biallelic loci, where $X_j = 0, 1$ denote alternative alleles and $\alpha_j > 0$ is the effect size at locus j. The trait is under directional selection on the island—the viability component of the fitness of an individual with trait value z is proportional to $e^{-\beta z}$, where β denotes the strength of viability selection. We will not explicitly model the mainland population but assume that trait values follow a normal distribution, or alternatively, that migrant genotypes are maximally deleterious on the island (see Section 2.2). Unless stated otherwise, we will also assume that the island is initially perfectly adapted (with $z = 0$ for each individual).

Individuals on the island mate assortatively, with trait z also serving as the basis for AM via female choice. We assume a Gaussian choice function, such that the probability of mating between a male and a female with trait values z_M and z_F is proportional to $e^{-\gamma(z_M - z_F)^2}$, where γ is the strength of assortment. In other words, females preferentially mate with males with trait values within a few $1/\sqrt{\gamma}$ of their own. Thus, the assortment trait is a "magic trait," which simultaneously influences mate choice and is under both natural and sexual selection, thereby generating both postzygotic and prezygotic barriers to gene flow.

We consider two different models of AM—allowing for sexual selection on both sexes (Model I) or only on males (Model II)—sometimes referred to as the "plant model" and the "animal model" of assortment (Kirkpatrick and Nuismer, 2004). The probability $M(z_M, z_F)$ of mating between a male and female with trait values z_M and z_F under the two models is

$$M(z_M, z_F) = \frac{e^{-\gamma(z_M - z_F)^2}}{\int\int P(z)P(y)e^{-\gamma(z-y)^2}\,dy\,dz} \qquad \text{Model I}$$

$$M(z_M, z_F) = \frac{e^{-\gamma(z_M - z_F)^2}}{\int P(z)\,e^{-\gamma(z-z_F)^2}\,dz} \qquad \text{Model II.}$$

Here, $P(z)$ is the trait value distribution just before mating. Note that under Model II, mating probabilities are normalized such that any female, regardless of trait value, mates with probability 1, while under Model I, females with rare phenotypes have lower mating probability. Thus, sexual selection acts only on males in the former case but on both sexes in the latter.

Effective migration rate at a neutral locus

Our analysis is based on effective migration rates (m_e)—defined as the rate at which neutral alleles entering a population via migration are incorporated into the resident gene pool (Barton and Bengtsson, 1986; Bengtsson, 1985, where "residents" are defined more precisely later. In our model, migrants and their descendants experience both viability and sexual selection and are less fit than residents. Consequently, in order to establish, neutral alleles must recombine away from migrant genetic backgrounds before these are eliminated by selection. Thus, m_e will vary along the genome, being lower at sites that are tightly linked to a selected locus or in genomic regions with a high density of selected loci. However, here we will focus on m_e at a neutral locus that is *unlinked* to any selected locus, since we are interested in quantifying the average or genome-wide reduction in gene flow.

Under rare migration ($m \ll 1$), the ratio m_e/m for an unlinked neutral allele, also called the gene flow factor g, is equal to the reproductive value (RV) of migrants relative to residents (Kobayashi et al., 2008). Here, RV refers to the long-term genetic contribution of the migrant in the recipient population (Barton and Etheridge, 2011; Fisher, 1999) and is given by

$$g = \frac{m_e}{m} = \prod_{i=0}^{\infty} \overline{W}_i, \tag{1}$$

where $\overline{W}_0$ denotes the average fitness of migrants relative to residents, and $\overline{W}_i$ the average relative fitness of ith generation descendants of migrants (see, e.g., Westram et al., 2022). For $m \ll 1$, individuals with recent immigrant ancestry are rare, so that migrants and their descendants mate primarily with residents. As a result, first-generation descendants of the migrants are F_1 hybrids, second-generation descendants are typically first-generation backcrosses (with residents), ith generation descendants are $(i-1)$th generation backcrosses (denoted by BC_{i-1}), and so on. Thus, computing m_e boils down to calculating the relative fitness of successive back-crosses.

In the following, we classify individuals on the island by the number of generations leading back to their most recent immigrant ancestor, that is, into F_1, BC_1, BC_2, up to BC_n (where n is arbitrary). All other individuals, that is, those with no migrant ancestor in the previous $n+1$ generations, are designated as "residents." We further assume trait values to be normally distributed *within* any group of individuals with the same level of recent migrant ancestry. In other words, the trait distributions $P_r(z)$, $P_1(z)$, ... $P_i(z)$, ... among residents, F_1 hybrids, ith generation descendants (who are BC_{i-1}), and so on, are assumed to be normal with means $\bar{z}_r, \bar{z}_1, \ldots \bar{z}_i, \ldots$ and variances $V_r, V_1, \ldots V_i, \ldots$, respectively (see Figure 1A; also Table 1). For generality, we also take the migrant trait value distribution to be normal with mean $\bar{z}_0$ and variance V_0. However, in the Results, we will only consider scenarios where the mainland is fixed for alleles locally deleterious on the island (so that $\bar{z}_0 = \sum_{j=1}^{L} \alpha_j$ and $V_0 = 0$).

Assuming normally distributed trait values is justified for traits influenced by a large number of loci of small effect. The inheritance of such traits is described by the infinitesimal model (Fisher, 1918), which states that trait values of the offspring of any two individuals are normally distributed about the mean of the parents, with a "within-family" variance V_*, which depends only on the genetic relatedness between parents, regardless of selection, nonrandom mating, etc. (Barton et al., 2017). We further assume that V_* depends only on the extent of migrant ancestry of the parental individuals and does not vary significantly across (for instance) different resident $\times$ F_1 parental pairs, all of which thus have approximately the same V_*. We denote the within-family variance by $V_{r,r}$ when both parents are residents, $V_{r,0}$ when one parent is a resident and the other migrant, and $V_{r,i}$ when one parent is a resident and the other an ith generation descendant of a migrant.

Then, we can express the distribution $P_i(z)$ in terms of the parental trait value distributions $P_r(z_1)$ and $P_{i-1}(z_2)$ (eq. 2a). Furthermore, we can express the mean fitness $\overline{W}_i$ of ith generation descendants (relative to residents) as an integral over the parental distributions (eq. 2b).

$$P_i(z) \propto \int\int P_r(z_1) P_{i-1}(z_2)\, e^{-\beta(z_1+z_2)} \times \left[\frac{M(z_1,z_2)+M(z_2,z_1)}{2}\right] \frac{e^{-\frac{(z-(z_1+z_2)/2)^2}{2V_{r,i-1}}}}{\sqrt{2\pi V_{r,i-1}}}\, dz_2\, dz_1 \tag{2a}$$

$$\overline{W}_i = \int\int \frac{e^{-\beta z_1}}{\int dz\, e^{-\beta z} P_r(z)} P_r(z_1) \frac{e^{-\beta z_2}}{\int dz\, e^{-\beta z} P_r(z)} P_i(z_2) \times \left[\frac{M(z_1,z_2)+M(z_2,z_1)}{2}\right] dz_2\, dz_1. \tag{2b}$$

In eq. 2a, z_1 and z_2 denote, respectively, the trait values of the resident parent and the parent who is an $(i-1)$th generation descendant of a migrant, with corresponding trait distributions $P_r(z_1)$ and $P_{i-1}(z_2)$. The term $e^{-\beta(z_1+z_2)}$ captures the effect of viability selection on the parents, while $M(z_1,z_2)$ (which is the probability of mating between a male and female with trait values z_1 and z_2, respectively) captures the effect of AM and sexual selection. Note that the nonresident parent may have a different probability of being chosen as a mate depending on whether it takes the female or male role during reproduction: this is captured by the two terms $M(z_1,z_2)$ and $M(z_2,z_1)$ (that are unequal under Model II). Finally, the last term gives the distribution of trait values of the offspring under the infinitesimal model; it captures the effect of recombination between parental genotypes and random segregation. Supplementary material A provides a detailed derivation of eq. 2.

Integrating over eq. 2a gives an expression for the mean and variance of trait values among the ith generation descendants in terms of the means and variances among $(i-1)$th generation descendants and among residents. This specifies a set of recursions which can be solved numerically to obtain $\bar{z}_i$, V_i, and $V_{r,i}$ (see SI, A). These fully specify the trait value distributions $P_i(z)$, which can be used to obtain the relative fitnesses $\overline{W}_i$ (using eq. 2b), which predict the gene flow factor g (eq. 1) and m_e.

However, in the main paper, we will derive a more approximate and intuitive expression for g by simply tracking the difference in trait means between residents and various groups

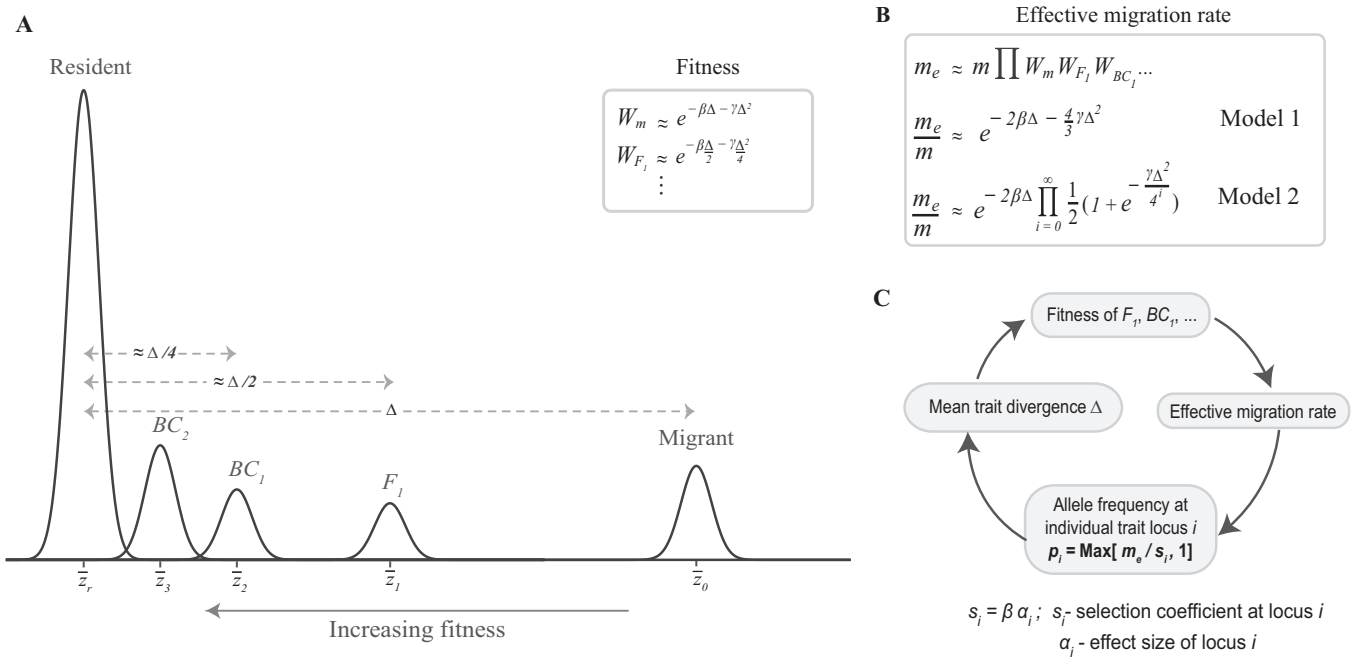

Figure 1. Schematic summarizing our theoretical approach for predicting mean trait divergence Δ (or allele frequency divergence per locus Y) using effective migration rates (m_e). (A) Distribution of trait values on the island is the sum of trait value distributions associated with residents, F_1s, BC_1s, and so on, where each such distribution is assumed to be approximately normal. Denoting the difference between trait means of migrants and residents by $\Delta = \bar{z}_0 - \bar{z}_r$, the difference between trait means of F_1s and residents is $\approx \Delta/2$, and more generally, between that of ith generation descendants (of migrants) and residents is $\Delta/2^i$. This allows us to calculate *average relative fitness* of F_1s, BC_1 etc. (inset). (B) The *gene flow factor* g (which describes the reduction in neutral gene flow at a site unlinked to any selected site) can be calculated from the average relative fitness of migrants and of individuals with recent migrant ancestry (F_1s, BC_1s), as in eq. 1. This gives approximate expressions for g under Model I (sexual selection on both sexes) and Model II (sexual selection only on males) (C) The *mean trait divergence* Δ can be calculated by first using m_e to predict the allele frequency p_i at trait locus $i = 1, \ldots, L$, then summing over loci to obtain the mean trait divergence Δ, then using this to predict relative fitnesses of F_1s, BC_1s and so on (as in A), and finally using these to predict the effective migration rate m_e (as in B). This kind of circular dependence, where m_e depends on Δ which depends on m_e (via allele frequencies), allows for a self-consistent solution for the mean trait divergence Δ.

(F_1s, BC_1s and so on) while neglecting phenotypic variance *within* any group. More concretely, we assume that the mean trait value of hybrid offspring is the average of the trait means of the parental subgroups. Thus, for example, F_1 hybrids are assumed to be midway between residents and migrants, giving $\bar{z}_1 \approx (\bar{z}_r + \bar{z}_0)/2$, which gives: $\bar{z}_1 - \bar{z}_r \approx (\bar{z}_0 - \bar{z}_r)/2 = \Delta/2$. Here, $\Delta = \bar{z}_0 - \bar{z}_r$ denotes the difference in the trait means of migrants and residents, which we refer to as mean trait divergence. It follows similarly that $\bar{z}_i - \bar{z}_r \approx (\bar{z}_{i-1} - \bar{z}_r)/2 = \Delta/2^i$ (see Figure 1A). Thus, in effect, every successive generation of backcrossing halves the mean phenotypic deviation of the (next-generation) backcross from the resident phenotype (Sachdeva, 2022; Zwaenepoel et al., 2024).

As we argue below and in SI, A, this simple argument holds as long as $\beta V_i \ll \Delta$ and $\gamma V_i \ll 1$ (for all i). Moreover, it follows from eq. 2b that under these conditions, the relative fitness of any group of descendants is: $\overline{W}_i \approx e^{-\beta(\bar{z}_i-\bar{z}_r)-\gamma(\bar{z}_i-\bar{z}_r)^2}$ for Model I (sexual selection on both sexes) and $\approx \frac{1}{2}e^{-\beta(\bar{z}_i-\bar{z}_r)}(1+e^{-\gamma(\bar{z}_i-\bar{z}_r)^2})$ for Model II (sexual selection only on males). Now, using $\bar{z}_i - \bar{z}_r = \Delta/2^i$, where Δ is the mean trait divergence between mainland and island, we obtain the following approximate expressions for the gene flow factor $g = \prod_{i=0}^{\infty}\overline{W}_i$ (see also Figure 1B):

$$g(\Delta) \approx e^{-2\beta\Delta-\frac{4}{3}\gamma\Delta^2} \quad \text{Model I} \qquad (3a)$$

$$g(\Delta) \approx e^{-2\beta\Delta}\prod_{i=0}^{\infty}\left(\frac{1+e^{-\gamma\Delta^2/4^i}}{2}\right) \quad \text{Model II.} \qquad (3b)$$

A more detailed derivation of eq. 3 is provided in SI, A. A striking feature of eq. 3 is that under both models of sexual selection, the gene flow factor can be expressed as a product of two terms—the first describing the reduction in RV of migrants due to viability selection, and the second due to sexual selection. The first term above, $e^{-2\beta\Delta}$, is the square of the viability component of migrant fitness relative to that of residents. The second term is related to the relative mating success of migrants and differs between the two models. For instance, under Model I, this term is simply the relative mating success of migrants raised to the power 4/3. These powers (of 2 or 4/3) emerge from the specific fitness and mating functions we consider. However, more generally, the fact that the viability and sexual selection components of g bear a simple relationship to the corresponding fitness components of migrants (or F_1s) is due to there being a simple relationship between individual fitness and long-term RV when fitness is polygenic.

What assumptions underlie our simple approximation for trait means, which is the basis of eq. 3? First, we ignore the fact that within any group of descendants, say F_1s, individuals that are phenotypically closer to residents have higher viability, causing the trait mean of BC_1s (the hybrid offspring of F_1s and residents) to be slightly shifted toward residents rather than exactly midway between the two parental groups.

Table 1. Key parameters and variables

Parameter/ Variable	Description
z	Additive magic trait; individual trait value $z = \sum_{j=1}^{L} \alpha_j X_j$, where $X_j = 0$ or 1 denote alternate alleles at locus j
α_j	Effect size at a locus j
L	Number of loci that influence magic trait
N	Population size
m	Rate of migration from mainland to island
β	Strength of viability selection on island; individual with trait value z has viability $\propto e^{-\beta z}$
γ	Strength of assortative mating
$M(z_M, z_F)$	Probability of mating between a male and female with trait values z_M and z_F; differs under the two models of assortative mating
s_j	Selection coefficient at locus j given by $s_j = \beta\alpha_j$; we consider equal-effect loci with $s_j = s$
m_e	Effective migration rate at any (equal-effect) trait locus
g	Gene flow factor $g = m_e/m$
Δ	Mean trait divergence between mainland and island, $\Delta = \sum_{j=1}^{L} \alpha_j(1-p_j)$; p_j is frequency of locally deleterious allele at locus j on island; mainland is fixed for the alternative allele
Δ_0	Maximum possible divergence between mainland and island, given by αL for equal-effect loci
Y	Allele frequency divergence per locus, $Y = \Delta/\Delta_0$, equals $1-p$ for equal-effect loci
$\beta\Delta_0, \gamma\Delta_0^2$	Scaled strengths of viability and sexual selection; amounts by which (log) fitness of migrants is reduced due to viability and sexual selection respectively, when $\Delta = \Delta_0$
m_c/s	Critical migration rate (relative to selection per locus) at which divergence Y becomes 0
Y_c	Allele frequency divergence associated with the tipping point
Quantities that appear in derivation of gene flow factor g	
$P_r(z), P_i(z)$	Trait value distribution among residents and ith generation descendants of migrants; $i = 0$ corresponds to migrants
$\bar{z}_r, \bar{z}_i$	Mean trait value among residents and ith generation descendants of migrants
V_r, V_i	Variance of trait values among residents and ith generation descendant of migrants
$V_{r,r}, V_{r,i}$	Within-family variance when one parent is a resident and the other a resident or an ith generation descendant of a migrant
$\overline{W}_i$	Mean fitness of ith generation descendants of migrants relative to residents

The magnitude of this shift is proportional to βV_1; thus, in ignoring the effects of viability selection *within* subgroups, we assume that $\beta V_i \ll \Delta$, where Δ is the mean trait divergence between mainland and island. As we argue in SI, A, under migration-selection balance, the various βV_i must be comparable to the migration rate m and can thus be neglected if $m \ll 1$.

Second, we ignore the effects of sexual selection within subgroups, which may lead to small differences in mating success among (say) F_1s, again slightly shifting the BC_1 trait mean toward one of the parental subgroups. Moreover, AM can also increase the phenotypic variance within each group (Crow and Felsenstein, 1968; Fisher, 1918; Wright, 1921), at least if sexual selection is weak, as under Model II (Kirkpatrick and Nuismer, 2004), further influencing the magnitude of these shifts. As we argue in Supplementary material A, both these effects can be ignored if $\gamma V_i \ll 1$, that is, if the preference function is much wider than the typical phenotypic spread within any subgroup. Thus, in summary, our simple approximation for trait means—$\bar{z}_i - \bar{z}_r \approx \Delta/2^i$ holds as long as $\beta V_i \ll \Delta$ and if $\gamma V_i \ll 1$. In effect, these two conditions amount to assuming that viability and sexual selection are strong enough to affect the survival and mating success of migrants and their F_1 and BC descendants relative to residents, but not strong enough to cause differential mating success *within* any group of descendants.

In summary, eq. 3 relates the gene flow factor $g = m_e/m$ at an unlinked locus to the mean trait divergence Δ between mainland and island at equilibrium, where Δ now depends on the allele frequency differences across all trait loci. In the following, we relate the allele frequency difference at any locus back to the effective migration rate m_e, thus allowing us to obtain the mean trait divergence in a self-consistent way (see Figure 1C).

Predicting allele frequency divergence at trait loci using m_e

We now develop approximations for allele frequencies at individual trait loci, assuming the mainland to be fixed for alleles that are deleterious on the island. Consider first a locus j with effect size α_j under *linkage equilibrium* (LE), that is, while

neglecting LD between the focal locus and all other trait loci. In SI, B, we show that under LE, sexual selection does not contribute to *direct* selection at any locus (at least under our assumed quadratic preference function), provided α_j is sufficiently small, that is, $\beta\alpha_j \ll 1$ and $\alpha_j \ll \beta/\gamma$. The latter condition can be rewritten as $\alpha_j/\Delta \ll (\beta\Delta)/(\gamma\Delta^2)$—this simply means that the relative contribution of any locus to trait divergence must be much smaller than the ratio of the sexual selection component of fitness to the viability selection component. Then, under LE, the equilibrium deleterious allele frequency p_j is simply m/s_j, where $s_j = \beta\alpha_j$ (Supplementary material B).

Following Sachdeva, 2022, we further assume that the main effect of LD between deleterious alleles is to reduce m_e at any locus. This can be justified as long as trait loci are unlinked or weakly linked so that LD between these breaks down much faster than allele frequencies change. Furthermore, if individual loci are weakly selected, then the effective migration rate at a trait locus is approximately equal to that at a neutral locus, so that in a large population, we have: $p_j \approx m_e/s_j \approx \frac{m}{s_j} g(\Delta)$. Here, the gene flow factor g is given by eq. 3 and captures the effect of both viability and sexual selection on migrants and their descendants.

Note that g depends on allele frequencies $\{p_j,\ j = 1,..L\}$ at all L loci via the mean trait divergence $\Delta = \sum_{j=1}^{L} \alpha_j(1-p_j)$. We can thus determine allele frequencies by numerically solving the L equations $p_j = (m/s_j)g(\Delta)$, all coupled via Δ (Zwaenepoel et al., 2024). However, here, we will focus on the simpler case of equal-effect loci, such that $\alpha_j = \alpha$ (and $s_j = s$) for all j. Then, in the absence of drift, equilibrium allele frequencies are equal across all loci (i.e., $p_j = p$), at least in parameter regimes where there is only one stable equilibrium. Thus, the mean trait divergence can be written as $\Delta = \alpha L(1-p)$. In the following, we will express our results in terms of $Y = \Delta/\Delta_0$, the trait divergence between the mainland and the island relative to the maximum possible divergence $\Delta_0 = \alpha L$. Note that for the case of equal-effect loci, we have: $Y = 1-p$, so that Y is also the mean allele frequency divergence per locus. It follows from eq. 3 that Y satisfies

$$Y \approx 1 - \frac{m}{s} e^{-2\beta\Delta_0 Y - \frac{4}{3}\gamma\Delta_0^2 Y^2} \qquad \text{Model I} \qquad (4a)$$

$$Y \approx 1 - \frac{m}{s} e^{-2\beta\Delta_0 Y} \prod_{i=0}^{\infty} \left(\frac{1 + e^{-\gamma\Delta_0^2 \frac{Y^2}{4^i}}}{2} \right) \qquad \text{Model II} \qquad (4b)$$

as long as a solution with $0 \le Y \le 1$ exists and is zero otherwise. Equation 4 can be solved numerically to obtain allele frequency divergence per locus Y or the trait divergence Δ. In the case of Model II, the product in eq. 4b converges rapidly and can be computed by taking the first ~ 20 terms.

Equation 4 is deterministic, implicitly assuming that $Ns \gg 1$, where N is the size of the island population. However, our basic approach can be generalized to account for genetic drift, by treating each frequency as a (continuous) *random* variable described by a probability density $\psi[p]$ (Sachdeva, 2022). Since a finite population subject to one-way migration requires nonzero mutation rates at trait loci in order to maintain long-term adaptive divergence, we allow for mutation at rate μ per individual per generation between alternative alleles at each locus. Then, under our approximation, the (unnormalized) equilibrium probability density $\psi[p]$ is given by

$$\psi[p|\Delta] = p^{2N\mu+2Nmg[\Delta]-1}(1-p)^{2N\mu-1}e^{-2Nsp} \qquad (5a)$$

$$\Delta/\Delta_0 = Y = \frac{\int_{p=0}^{1} p\,\psi[p|\Delta]\,dp}{\int_{p=0}^{1} \psi[p|\Delta]\,dp}. \qquad (5b)$$

Equation 5a is simply the allele frequency distribution at a single locus at migration-selection-mutation-drift equilibrium, as predicted by the diffusion approximation (Wright, 1937), but with m replaced by $m_e = m\,g[\Delta]$. As before, the effective migration rate m_e (or equivalently the gene flow factor g) is a function of the trait divergence Δ and is given by eq. 3. We can obtain Δ, in turn, by summing over allele frequencies at all trait loci. With equal-effect loci, we have: $\Delta = \Delta_0 Y$, where Y, the expected allele frequency divergence per locus, is obtained by integrating over $\psi[p]$ (eq. 5b), thus allowing us to self-consistently solve for Δ (as in the deterministic case).

Deterministic simulations

In the main paper, we analyze the deterministic limit and test our approximations (eqs 3 and 4) against deterministic simulations based on the hypergeometric model, which describes the inheritance of a quantitative trait influenced by equal-effect loci (Barton, 1992; Doebeli, 1996). In each generation, migration is followed by viability selection, which is followed by assortative mating (involving sexual selection on one or both sexes), and production of offspring via free recombination between parental genotypes. The mainland is fixed for alleles that are locally deleterious on the island. Additionally, unless stated otherwise, simulations are initialized with the island fixed for the locally adaptive allele at each trait locus.

Note that with equal-effect loci, the trait value z of any individual is just αj, where j is the number of locally deleterious alleles it carries. Supplementary material C specifies the recursions that describe how the distribution $P(j)$ (or alternatively, $P(z)$) changes over one generation under the combined effects of migration, (viability and sexual) selection, AM, and random segregation. These recursions for $P(j)$ are iterated until equilibrium is attained, and allele frequency divergence per locus Y calculated using: $Y = \frac{1}{L}\sum_{j=0}^{L}(L-j)P(j)$. This can then be compared with theoretical predictions (eq. 4).

Individual-based simulations of finite populations (which are used to explore the effects of genetic drift on divergence) are described in Supplementary material D.

Results

We now use predictions based on effective migration rates to investigate the combined effects of migration, viability and sexual selection, and assortative mating on the equilibrium trait divergence between mainland and island as well as on the genome-wide reduction in neutral gene exchange (as measured by the gene flow factor). In the main paper, we focus on

the deterministic limit of the model; the effects of genetic drift are examined in Supplementary material D. We first quantify how mean trait divergence declines with increasing migration (which is parameterized by m/s, migration rate relative to selective effect per locus), for different strengths of viability and sexual selection against migrants. This allows us to identify a critical migration threshold m_c beyond which adaptive divergence is completely swamped by gene flow, that is, Y becomes zero. Next, we ask: how strong do viability and sexual selection have to be to shift this swamping threshold to *above* that for a single divergently selected locus? Finally, we examine the relative contributions of viability and sexual selection to RI under different parameter regimes, by using the increase in F_{ST} at an arbitrary site (unlinked to any trait locus) as a proxy for the genome-wide barrier effect.

Throughout, we quantify the strength of viability and sexual selection in terms of $\beta\Delta_0$ and $\gamma\Delta_0^2$, which denote, respectively, the reduction in log fitness of migrants (relative to residents) due to viability and sexual selection under conditions of maximum divergence between the mainland and island, that is, when $\Delta = \Delta_0$. If traits are highly polygenic (large L and small effect sizes α), then in the deterministic limit, divergence (as measured by $Y = \Delta/\Delta_0$) depends essentially on the composite parameters m/s, $\beta\Delta_0$ and $\gamma\Delta_0^2$, where $\Delta_0 = \alpha L$ (see eq. 4). However, for smaller L (say tens of loci), divergence levels may be sensitive to the exact genetic basis of the trait, that is, depend on α and L separately (Supplementary material E). In the main text, we focus only on the large L limit (where eq. 4 applies). In addition, we assume a scenario of secondary contact where mainland and island are initially maximally diverged; other initial conditions (with partial divergence) are explored in Supplementary material F.

Effect of viability and sexual selection on adaptive divergence

Figure 2A–F show Y, the allele frequency divergence per locus (or equivalently, the trait divergence between mainland and island relative to the maximum possible divergence) as a function of m/s, under the two models of AM in the deterministic limit. For each model, we show results for $\beta\Delta_0 = 0.2, 0.5, 1$ (stronger viability selection from left to right). Furthermore, for each $\beta\Delta_0$, we contrast random mating (gray) with populations with increasing assortment ($\gamma\Delta_0^2 = 0.5$, 1 and 1.5; different colors), which generates increasing levels of sexual selection on both sexes (Model I; top) or only on males (Model II; middle). The analytical predictions obtained by solving eq. 4 (lines) match well with the results of deterministic simulations of a trait influenced by $L = 80$ loci (points) unless net selection (viability and/or sexual selection) is very strong; see, e.g., red curves corresponding to $\gamma\Delta_0^2 = 1.5$ in Figure 2E and F (with $\beta\Delta_0 = 1$). This discrepancy between simulations and theory becomes smaller with increasing number of trait loci (Supplementary material E).

Thus, there is a wide range of parameter values for which simple approximations based on m_e (eq. 4) accurately predict equilibrium divergence. Note that these approximations only account for the lower RV of migrants due to sexual (and viability) selection but ignore other effects of AM—such as the increased variance among residents, F_1s, etc., and the increased probability of mating between individuals with recent migrant ancestry. That there is, nonetheless, close agreement between theory and simulations suggests that, in our model, AM strengthens divergence by generating additional (sexual) selection against migrants and their descendants. This reduces m_e, thus increasing the genome-wide barrier effect and facilitating further divergence (see also *Discussion*).

As evident from Figure 2G–I, this reduction in m_e (or equivalently g) is stronger under Model I (where sexual selection acts on both sexes) as compared with Model II (sexual selection only on males) and also depends on existing levels of divergence (which in turn depend on the strength of migration and viability selection). Figure 2 also highlights how migration affects divergence differently in parameter regimes characterized by strong versus weak selection against migrants. When sexual selection (due to assortment) and viability selection are weak, divergence decreases *smoothly* with increasing m/s, going to zero at a critical threshold $m_c/s = 1$, regardless of the actual value of $\beta\Delta_0$ and $\gamma\Delta_0^2$ (e.g., in Figure 2B). Note that $m_c/s = 1$ is also the critical migration threshold for loss of adaptation at a single divergently selected locus. Thus, this threshold remains unchanged even when divergence involves many loci, as long as total selection on these is weak.

In contrast, with strong viability and/or sexual selection, divergence first decreases mildly with increasing migration but then exhibits an *abrupt* collapse once it crosses a threshold Y_c (at a migration level $m/s \gtrsim 1$). Such a "tipping point," defined as a discontinuous change in divergence (though not necessarily to $Y = 0$), can be observed in Figure 2C and D for higher assortment and in Figure 2E and F at all levels of AM. We can use eq. 3 to obtain expressions for Y_c, the allele frequency divergence threshold associated with tipping points, under the two models of AM (details in Supplementary material G)

$$Y_c = \frac{(4\gamma\Delta_0^2 - 3\beta\Delta_0) + \sqrt{(3\beta\Delta_0 + 4\gamma\Delta_0^2)^2 - 24\gamma\Delta_0^2}}{8\gamma\Delta_0^2} \quad \text{Model I} \tag{6a}$$

$$Y_c = 1 - \frac{1}{2\beta\Delta_0 + 2\gamma\Delta_0^2\, Y_c \sum_{i=0}^{\infty} \frac{4^{-i}}{1+e^{\gamma\Delta_0^2 (Y_c^2/4^i)}}} \quad \text{Model II.} \tag{6b}$$

For Model II, eq. 6b specifies a transcendental equation for Y_c, which can be solved numerically (e.g., by approximating the sum by the first $\sim$ 20 terms). Furthermore, in SI, G, we show that the migration threshold associated with such a tipping point is: $m/s = (1 - Y_c)/g(\Delta_0 Y_c)$, where g, the gene flow factor, is given by eq. 3, and $\Delta_0 Y_c$ is the mean trait divergence at the tipping point.

The threshold Y_c can also be thought of as the minimum allele frequency difference per locus required to "lock in" divergently selected alleles across the genome into distinct combinations that can be stably maintained by selection despite gene flow. Divergence levels lower than Y_c would result in an insufficient genome-wide barrier to gene flow, leading to a further decrease in divergence, further increasing m_e and so on, thus inducing a tipping point. Interestingly, even though the tipping point occurs at a certain level of migration (see, e.g., Figure 2A–F), the divergence threshold Y_c associated with the tipping point is *independent* of this migration rate and depends only on the strengths of viability and sexual selection (eq. 6).

In addition to generating tipping points, strong viability or sexual selection (or both) can also increase the critical

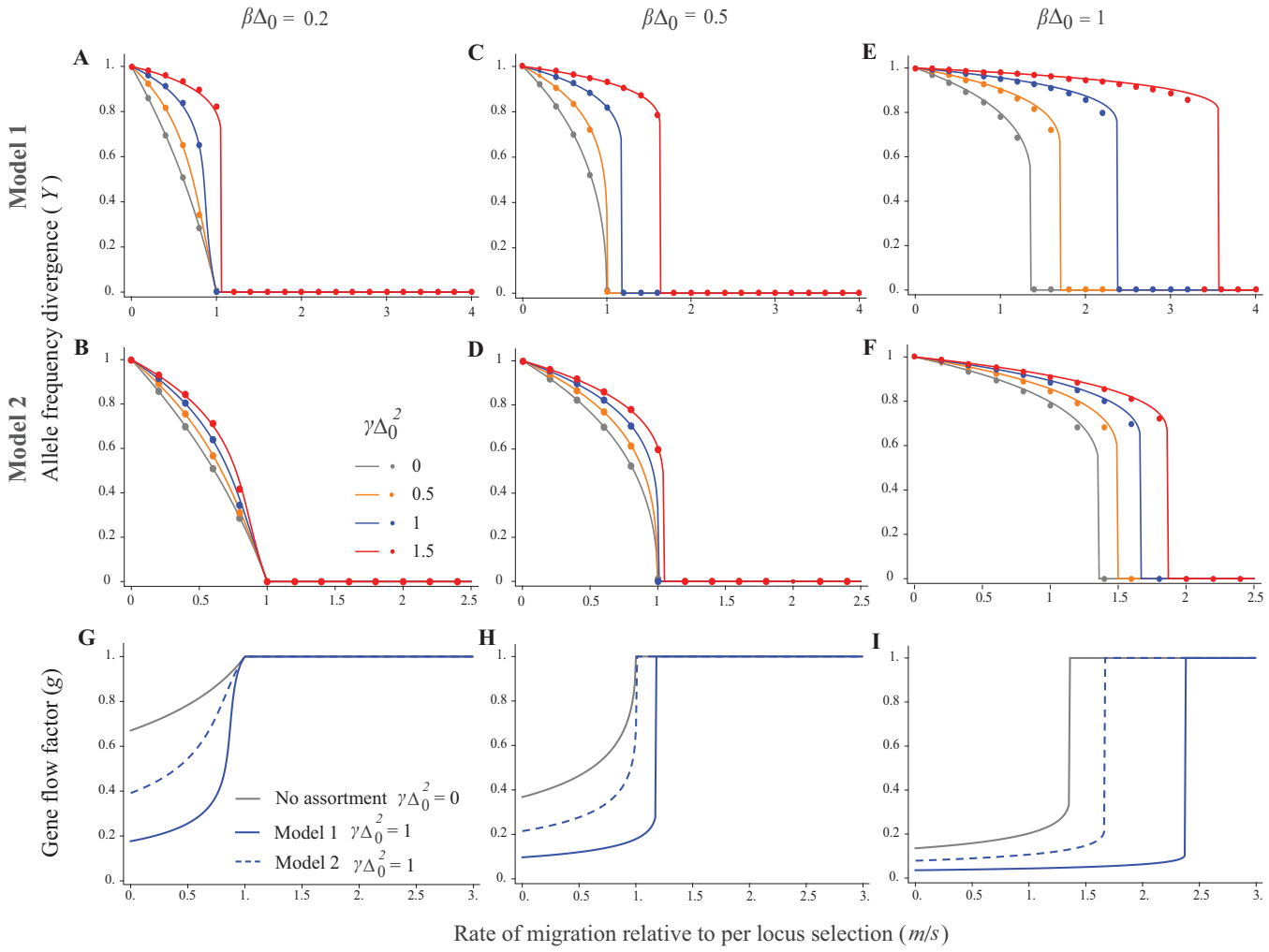

Figure 2. Allele frequency divergence per locus Y and gene flow factor g as a function of m/s, the migration rate relative to selection per locus. The top and middle rows, respectively, depict divergence levels for Model I (sexual selection on both sexes) and Model II (sexual selection only on males). Different subfigures within each row correspond to different strengths of viability selection ($\beta\Delta_0 = 0.2, 0.5, 1$ from left to right); different colors within each plot depict different strengths of AM and sexual selection ($\gamma\Delta_0^2 = 0$, 0.5, 1, 1.5 shown in gray, orange, blue, and red, respectively). Solid lines show theoretical predictions (obtained by numerically solving eq. 4), while dots represent the results of deterministic simulations of the hypergeometric model with $L = 80$ loci underlying the polygenic trait. Increasing viability and sexual selection cause sharper thresholds ("tipping points") for loss of divergence as well as an increase in the critical migration rate at which divergence is lost. The bottom row depicts theoretical predictions for the gene flow factor g for random mating (gray) vs. assortatively mating populations under Models I and Models II (solid vs. dashed lines), assuming $\gamma\Delta_0^2 = 1$. The gene flow factor and m_e are more strongly reduced under Model I than under Model II.

migration threshold for loss of divergence *above* the single-locus threshold $m_c/s = 1$ (see, e.g., Figures 2E and F). In other words, if selection against migrants and their descendants is sufficiently strong, then polygenic divergence can be maintained at migration levels at which a single divergently selected locus (in the absence of LD) would have been swamped.

Both tipping points and increased swamping thresholds may be explained as follows: higher levels of migration reduce adaptive divergence between mainland and island, thereby increasing m_e (see eq. 3) and weakening multilocus selection against locally deleterious alleles, which increases their frequency—further reducing adaptive divergence and increasing m_e, which finally results in the swamping of locally adaptive alleles above a certain migration threshold. Crucially, the positive feedback between loss of divergence at individual loci and increase in m_e across the genome is stronger when net selection against migrant phenotypes (either viability or sexual selection) is higher. In the next section, we will explore how strong viability and sexual selection need to be to produce these effects.

Note that while Figure 2 and the analyses below pertain to the deterministic model, the basic results also hold for a finite population of size N, provided Ns is large. For instance, tipping points occur under both models of AM if $Ns \gtrsim 5$, for moderately strong (viability plus sexual) selection (Supplementary material D). Moreover, theoretical approximations based on m_e (eq. 5) also furnish reasonably accurate predictions for divergence levels in finite populations (Figure S1, Supplementary material).

When does assortative mating and sexual selection lead to tipping points and higher swamping thresholds?

We first illustrate the various thresholds described above using a concrete example assuming weak viability selection ($\beta\Delta_0 =$

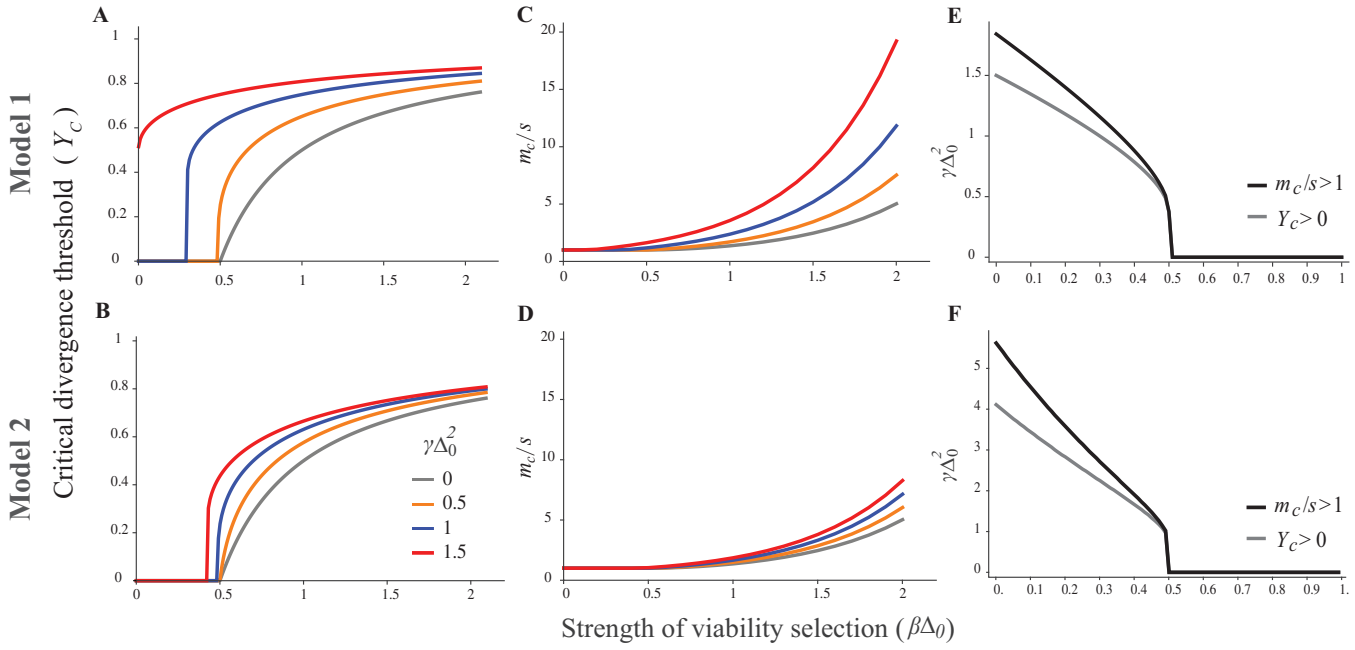

Figure 3. Deterministic predictions for swamping thresholds and tipping points. (A) and (B) Critical allele frequency divergence Y_c below which a tipping point occurs (i.e., divergence decreases sharply) vs. $\beta\Delta_0$, the strength of viability selection. (C) and (D) Critical migration rate m_c/s at which divergence is completely lost vs. $\beta\Delta_0$. The different colors show results for different levels of AM and sexual selection ($\gamma\Delta_0^2$ = 0, 0.5, 1 and 1.5). Upper panel (A, C, E) shows results for Model I (sexual selection on both sexes) and lower panel for Model II (sexual selection only on males). In panels A and B, parameter combinations with $Y_c = 0$ are those for which divergence decreases smoothly with increasing migration, i.e., there is no tipping point. In panels C and D, parameter combinations with $m_c/s = 1$ are those for which viability and sexual selection are too weak to shift the swamping threshold above the single-locus threshold. (E) and (F) Gray curves show the minimum level of sexual selection (as measured by $\gamma\Delta_0^2$) required for nonzero Y_c, i.e., to generate tipping points in divergence, as a function of $\beta\Delta_0$, the strength of viability selection. Black curves show the minimum level of sexual selection ($\gamma\Delta_0^2$) required for $m_c/s > 1$, i.e., to shift the swamping threshold above the single-locus threshold, as a function of $\beta\Delta_0$. Panels E and F correspond to Model I and II, respectively. All results in this figure show (large L) theoretical predictions obtained from eqs 3 to 6.

0.2) under Model I (sexual selection on both sexes). For *weak* AM and sexual selection (in this example, $\gamma\Delta_0^2 < 1.2$), divergence decreases smoothly with increasing migration and is completely swamped at $m_c/s = 1$—this behavior is qualitatively similar to that of a single divergently selected locus. For *intermediate* assortment (here, $1.2 < \gamma\Delta_0^2 < 1.4$), increasing migration leads to a tipping point or discontinuous change in divergence: this occurs once allele frequency divergence per locus approaches a threshold Y_c (approximately predicted by eq. 6) and involves a strong reduction in the genome-wide barrier effect. However, in this intermediate assortment regime, tipping points still occur at migration rates lower than the single-locus swamping threshold $m_c/s = 1$. For instance, for $\gamma\Delta_0^2 = 1.3$, the tipping point occurs at $m/s \approx 0.95$ and is associated with $Y_c \sim 0.6$: thus, a tiny increase in m/s (say from 0.949 to 0.95) causes allele frequency divergence per locus to fall from 0.6 to 0.1 (Figure S5). A further increase in migration further reduces divergence, and complete swamping occurs (as before) at $m_c/s = 1$. However, with even *stronger* assortment (in this example, $\gamma\Delta_0^2 > 1.4$), the genome-wide barrier effect becomes strong enough to maintain divergence beyond $m/s = 1$, so that the tipping point now occurs at $m_c/s > 1$. Furthermore, divergence is completely swamped (Y goes to zero) at the tipping point. Thus, in this strong assortment regime, tipping points and swamping thresholds coincide and occur at a critical migration threshold that exceeds the single-locus threshold (see also Figure S5). This is in contrast to the intermediate assortment regime—where the tipping point occurs (i.e., divergence falls to a low but nonzero level) at a migration rate lower than the swamping threshold.

We now ask: in what parameter regimes do we observe these qualitatively different behaviors? Figure 3A and B shows the divergence threshold Y_c associated with tipping points (discontinuous changes in divergence), while Figure 3C and D shows the critical migration threshold m_c/s beyond which divergence is completely swamped, as a function of the strength of viability selection (measured as $\beta\Delta_0$). As discussed above, the migration threshold associated with the tipping point is the same as the swamping threshold m_c/s if assortment is strong. Figure 3A–D shows Y_c and m_c/s for the two models of AM; colors in each plot correspond to different $\gamma\Delta_0^2$, which quantifies the strength of sexual selection (due to AM). These predictions all follow from eqs. 3–6 (see Supplementary material G for details).

Under sufficiently strong viability selection ($\beta\Delta_0 > 0.5$), increased swamping thresholds ($m_c/s > 1$) arise even in the absence of AM, as shown by the gray lines in Figure 3C and D (see also Sachdeva (2022)). Thus, in this regime, AM and sexual selection further increase the swamping threshold m_c/s (beyond 1) as well as the critical level of divergence Y_c that can be stably maintained. This can be explained, as before, in terms of the effects of sexual selection on m_e and the overall genome-wide barrier to gene flow. As expected, AM has a stronger effect in Model I (where sexual selection is stronger) than in Model II. For example, for $\beta\Delta_0 = 1$, AM with strength $\gamma\Delta_0^2 = 1$ increases the critical migration threshold (m_c/s) from 1.36 (under random mating) to 2.37 under Model I and 1.66 under Model II. Note also that AM makes it harder to maintain intermediate levels of divergence, with divergence becoming unstable and collapsing once mean allele

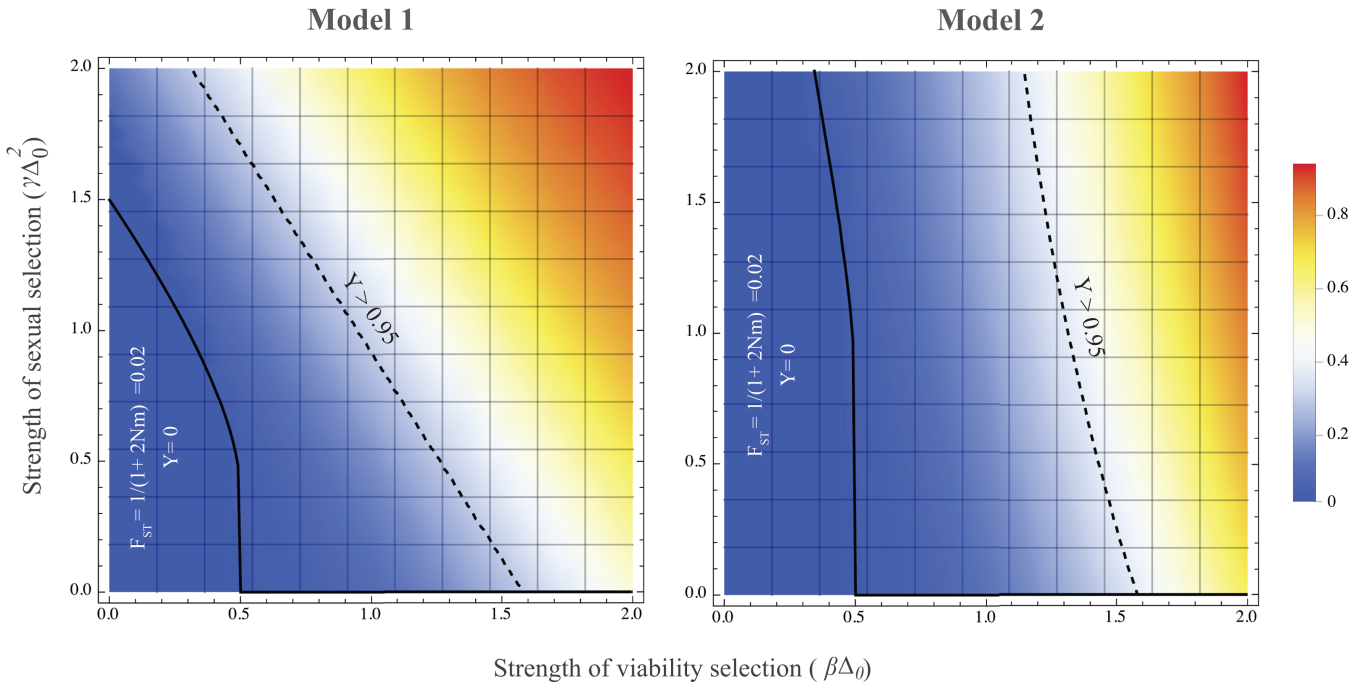

Figure 4. Heatmaps depicting F_{ST} at an unlinked neutral locus for different values of $\beta\Delta_0$ and $\gamma\Delta_0^2$ (which parameterize viability and sexual selection, respectively) for Model I (sexual selection on both sexes) and Model II (sexual selection only on males) of assortative mating, assuming $m/s = 1$ and $2Nm = 49$. The color bar on the right shows F_{ST} values ranging from $F_{ST} = 0$ to 1. Parameter combinations to the left of the solid line are those for which there is no trait divergence (i.e., $Y = 0$) so that $F_{ST} = 1/(1+2Nm) = 0.02$; parameters to the right of this line allow for divergence, so that $F_{ST} = 1/(1+2Nm\,g\,[\Delta_0 Y])$, where Y is obtained by solving eq. 4. Parameters to the right of the dashed line are those for which $Y > 0.95$: in this regime, stronger viability or sexual selection increases the genome-wide barrier effect and F_{ST} without significantly affecting divergence at trait loci (which is close to its maximum possible value).

frequency difference per locus approaches 0.75 under Model I and 0.66 under Model II (for $\beta\Delta_0 = 1$). In contrast, under random mating, we have $Y_c = 0.5$, so that somewhat lower levels of divergence can be stably maintained between the mainland and island, albeit at lower migration rates.

The situation is somewhat different if $\beta\Delta_0 < 0.5$; now, viability selection by itself (i.e., in the absence of AM) is too weak to generate tipping points or shift the swamping threshold m_c/s. However, sufficiently strong sexual selection due to AM will lead to one or both. More specifically, given viability selection $\beta\Delta_0 < 0.5$, we can determine an assortment threshold, that is, a minimum value of $\gamma\Delta_0^2$ beyond which tipping points occur (i.e., we observe a nonzero Y_c in Figure 3B and D), and a second threshold beyond which critical migration rates become higher than the single locus threshold (m_c/s exceeds 1 in Figure 3A and C); see Supplementary material G for details. These assortment thresholds are depicted by gray and black curves, respectively, in Figure 3E and F.

As expected, much higher levels of AM are required to generate tipping points and increase swamping thresholds when viability selection is weak, and when sexual selection acts only on males (instead of both sexes). For instance, with $\beta\Delta_0 = 0.2$, we have $m_c/s > 1$ only if $\gamma\Delta_0^2$ exceeds 1.41 under Model I and 3.58 under Model II (see Figure 3E and F). However, the sex-averaged mating success of migrants relative to residents is $e^{-\gamma\Delta_0^2} \sim 0.24$ (for $\gamma\Delta_0^2 = 1.41$) under Model I and and $(1+e^{-\gamma\Delta_0^2})/2 \sim 0.512$ (for $\gamma\Delta_0^2 = 3.58$) under Model II, both calculated by assuming maximum divergence between mainland and island. Thus, critical assortment thresholds are associated with much stronger sexual selection on migrants under Model I (sexual selection on both sexes) than Model II, despite AM being weaker in the former case.

Effect of viability and sexual selection on neutral gene flow

In the previous section, we have shown that approximations based on m_e accurately predict long-term adaptive divergence between the mainland and island under AM and sexual selection. In essence, divergent selection at very many loci (whether due to viability or sexual selection) results in a genome-wide reduction in gene flow, which further strengthens divergence across the genome. As discussed above, this genome-wide reduction can be quantified via $g = m_e/m$, the gene flow factor at an unlinked locus, which may be viewed as a measure of RI between hybridizing populations (see Westram et al. (2022)). Moreover, g is also related to commonly used measures of neutral differentiation such as F_{ST}, which depends on both the number of migrants, Nm, and their RV (which is equal to g). More concretely, at equilibrium, neutral F_{ST} between the mainland and island is $F_{ST} \sim 1/(1+2Nm_e) = 1/(1+2Nm\,g)$ on average.

We now quantify the extent to which viability and sexual selection reduce gene flow across the genome in a scenario with high migration ($2Nm = 49$). Note that in the absence of divergent selection, such high levels of gene flow would erase most neutral differences between mainland and island, resulting in $F_{ST} = 0.02$. However, strong enough selection can maintain adaptive divergence despite high migration, thus suppressing gene flow and increasing genome-wide F_{ST}. Figure 4 illustrates this by plotting F_{ST} as a function of $\beta\Delta_0$ and $\gamma\Delta_0^2$

for $m/s = 1$, under the two models of AM. These figures are generated by solving for the allele frequency divergence per locus Y (using eq. 4) for each combination of $\beta\Delta_0$ and $\gamma\Delta_0^2$, then using this to compute the gene flow factor g (via eq. 3), and finally computing $F_{ST} = 1/(1 + 2Nmg)$.

In each plot, the region to the left of the solid curve shows parameter combinations for which adaptive divergence is lost ($Y = 0$) at $m/s = 1$, so that $m_e = m$ and $F_{ST} = \frac{1}{1+2Nm} = 0.02$. As before, increasing $\beta\Delta_0$ and $\gamma\Delta_0^2$ (which correspond to stronger viability and sexual selection, respectively) allow nonzero adaptive divergence to be maintained, thereby reducing m_e and increasing F_{ST}. The dashed curve in each plot depicts parameter combinations for which mean allele frequency divergence is $Y = 0.95$, which corresponds to a gene flow factor of $g \approx \frac{1-Y}{m/s} = 0.05$ and an F_{ST} value of $\frac{1}{1+2Nmg} \approx 0.29$ under either model of AM. To the right of this curve, that is, with even stronger viability and/or sexual selection, there is a further increase in F_{ST}, which is now *not* due to an increase in adaptive divergence (which is close to its maximum possible value). Instead higher levels of F_{ST} in this parameter regime reflect lower viability and mating success of (nearly maximally diverged) migrants, which further reduces neutral gene exchange between mainland and island.

We can also ask: do changes in the strength of viability and sexual selection multiplicatively (i.e., independently) affect gene flow (as measured by g) or are their combined effects stronger (or weaker) than expected from their individual effects? More concretely, consider a scenario with moderately strong viability and sexual selection ($\beta\Delta_0 = \gamma\Delta_0^2 = 0.5$), $m/s = 1$, so that mean allele frequency divergence is $Y = 0.36$ (from eq. 4) and $g = 0.64$ (from eq. 3) under Model I. A 20% increase in *either* viability or sexual selection, that is, increasing $\beta\Delta_0$ to 0.6 while keeping $\gamma\Delta_0^2$ fixed at 0.5 (or vice versa) causes g to fall to 55% (or 74%) of its original value. Now, if viability and sexual selection were to independently reduce gene flow, then we would expect g to decrease by a factor of $0.55 \times 0.74 = 0.39$, that is, to 39% of its original value in response to a 20% increase in *both* components of selection ($\beta\Delta_0 = \gamma\Delta_0^2 = 0.6$). Instead, g decreases to 43% of its original value. Thus, in this example, the two kinds of reproductive barriers (lower survival and lower mating success of immigrants and their descendants) cause a weaker reduction in gene flow than if they were to act independently.

Such nonindependent effects arise because the gene flow factor is a product of two terms—one due to viability and the other due to sexual selection (see eq. 3), both of which depend on allele frequency divergence Y, which in turn is influenced by both components of selection. Thus, the strongest nonmultiplicative effects emerge in parameter regimes where viability and sexual selection are strong enough to significantly influence divergence levels but not so strong as to drive divergence to its maximum possible value. In the latter scenario, that is, as Y approaches 1 (to the right of the dashed curves in Figure 4), the effect of viability and sexual selection again becomes multiplicative.

Discussion

While it has long been recognized that sexual selection can maintain interspecific differences, questions remain as to its importance relative to other processes during speciation (Safran et al., 2013). Sexual selection varies considerably across species and even across environments within a species or over time (Magurran and Ramnarine, 2004; Rosenthal, 2013; Schumer et al., 2017), making it difficult to identify broad patterns. Moreover, sexual selection typically acts together with other kinds of selection against heterospecifics and hybrids (e.g., due to ecological mismatch or expression of genetic incompatibilities), making it difficult to disentangle the contributions of different processes to RI. This only underscores the broader challenges of quantifying RI—an issue that has recently attracted considerable attention (Westram et al., 2022).

Here, we examine some of these issues in the context of a polygenic "magic" trait that is under divergent ecological selection across populations while also mediating AM and sexual selection. In such a scenario, long-term divergence depends crucially on LD between trait loci. Such LD is, in turn, a consequence of both (natural and sexual) selection and assortment, making it challenging to model. Previous analyses have relied on one of two approaches—either focusing on how trait variances are affected by selection and assortment while largely ignoring genetic details (e.g., Doebeli, 1996; Kondrashov and Shpak, 1998), or explicitly modeling LD between sets of loci (Barton and De Cara, 2009; Kirkpatrick, 2000), but assuming that it is weak (to ensure tractability). Here, we employ a novel approach based on effective migration rates that bridges phenotypic descriptions (involving trait means and variances) with genic descriptions (based on divergence at individual selected sites).

An advantage of our approach is that it provides an economical description of tipping points in terms of just allele frequency differences between populations rather than a plethora of LD measures. The key idea behind our approach is that LD between introgressing alleles breaks down rapidly when these are unlinked or loosely linked (a standard assumption in quantitative genetics), allowing us to represent its effects via an effective migration rate m_e (or alternatively, the gene flow factor $g = m_e/m$) over the longer timescales over which allele frequencies change. The gene flow factor, being the average RV of migrants, is a composite measure of various processes—prezygotic and postzygotic—that affect the fitness of migrants and their descendants. In particular, it captures both the prezygotic effects of AM—which causes fewer F_1 hybrids to be produced (due to sexual selection against migrants) and its postzygotic effects—as reflected in the lower mating success of F_1s and later-generation hybrids (again, due to sexual selection).

As we show here, theory based on m_e accurately predicts divergence across a range of parameters, including when LD is strong enough to generate so-called tipping points (Nosil et al., 2017), but also when genetic drift is strong enough to wash away these tipping points (see SI, D). Moreover, it captures the consequences of sexual selection on one versus both sexes (Model I vs. II). These models show qualitatively similar behaviors—tipping points and/or shifted swamping thresholds, which, however, occur at much higher levels of assortment under Model II (compared with Model I) due to net (sex-averaged) sexual selection being weaker in this case. This again highlights the fact that it is sexual selection (rather than AM per se) that influences barriers to gene flow in our model.

We also show that, to a good approximation, g is a product of two terms—one reflecting viability selection and the other sexual selection on migrants and their descendants (see eq. 3).

This is in line with previous work that quantifies sexual and natural selection in terms of the probabilities of conspecific versus heterospecific mating, or the fitness of offspring from different types of mating, but assumes that the two selection components multiplicatively determine the total barrier to gene flow (Sobel and Chen, 2014; Ramsey et al., 2003). Note, however, that in our model, the two components (due to viability and sexual selection) both depend on the existing level of divergence Δ and are thus not independent. For instance, stronger AM and sexual selection typically increase divergence, which also reduces the (relative) viability of migrants and their descendants, thus further strengthening the barrier effect of viability selection, even when there is no change in the strength of viability selection. This suggests that measurements of RI are highly context- and state-dependent, making it difficult to extrapolate from lab measurements or between replicate hybrid zones.

Nevertheless, in theory, eq. 3 provides an unambiguous way of quantifying the contributions of natural and sexual selection to RI. In practice, this requires estimates of fitness components of individuals with different levels of migrant ancestry, which are only available in a handful of well-studied populations with multigenerational pedigrees (Bérénos et al., 2014; Chen et al., 2019). However, such populations are necessarily spatially restricted and show very little divergence or RI. More typically, we may have indirect fitness estimates for hybrids (and less commonly, for backcrosses and recombinants) from hybrid zones between divergent ecotypes. It is an open question whether combining these with experimental approaches, for example, reciprocal transplant or mate choice experiments (that individually measure viability or mating success) could provide reliable estimates of fitness components in natural populations, thus allowing us to disentangle the contributions of natural and sexual selection to RI.

Our work also has implications for the interplay between assortative mating and sexual selection during divergence with gene flow. The distinction between the two has been highlighted in earlier work (Kirkpatrick and Nuismer, 2004; Polechová and Barton, 2005; Servedio and Bürger, 2014), which points out that sexual selection can reduce the mating success of outlier individuals, thus constraining genetic variance and reducing the potential for divergence (Kirkpatrick and Nuismer, 2004). In contrast, pure assortment without sexual selection always increases variance, thus facilitating divergence.

The situation is somewhat different following secondary contact between diverged populations: now, sexual selection against migrants reduces introgression of deleterious alleles. This effect is only strengthened by assortative mating (based on ancestry), which increases LD between introgressing alleles, causing them to be eliminated more effectively. In recent work, Muralidhar et al. (2022) provide a rough estimate of the effect of AM following a pulse of admixture in a scenario where individual viability decreases in proportion to introgressed ancestry. Their argument is as follows: the change in introgressed allele frequency per generation (due to viability and/or sexual selection) is proportional to the variance of introgressed ancestry across individuals. In an assortatively mating population with correlation coefficient ρ between mates (where ρ is a measure of the strength of AM), the variance in introgressed ancestry declines by a factor $\sim (1+\rho)/2$ per generation, *slower* than it would under random mating, allowing for more efficient selective purging of introgressing alleles. It then follows that AM *by itself* (as a process that is distinct from sexual selection) increases net purging by a factor of $1/(1-\rho)$ (Muralidhar et al., 2022). This argument implicitly assumes that sexual selection is weak and does not cancel out the variance-increasing effect of AM; this assumption would break down, for instance, under our Model I (see also Kirkpatrick and Nuismer, 2004)

The conclusions of Muralidhar et al. (2022) differ from ours—in particular, we show that divergence is shaped essentially by sexual selection on various subgroups (i.e., F_1s, BC_1s, etc.), with little to no effect of AM (e.g., on within-subgroup variances). What might explain these differing conclusions? Muralidhar et al. (2022) analyze the consequences of a single admixture event that replaces a sizable fraction of the native population by migrants from a diverged population. In this case, individuals with recent migrant ancestry are sufficiently common to mate assortatively with one another—this causes LD between introgressing alleles to persist longer, thus allowing selection to eliminate them efficiently. In contrast, we consider ongoing migration at rate m and focus on the long-term equilibrium between selection and migration. In this case, long-term adaptive divergence requires m_e to be lower than the typical per locus selective effect s, so that m is at most a few times larger than s. Thus, migration is sufficiently low that individuals with recent migrant ancestry mate predominantly with residents rather than with each other. Then, introgression depends essentially on the mating success of (or alternatively, sexual selection on) various hybrids (F_1, BC_1, etc.) relative to residents. We emphasize that assuming low migration rates ($m \ll 1$) does not imply that neutral divergence between populations is high, since the latter depends on the number of migrants Nm per generation, which may be large. Nor does it imply high levels of adaptive divergence (see, e.g., Figure 2); indeed, this can be arbitrarily low, depending on m/s, and the total strength of viability and sexual selection.

The preceding discussion highlights how the role of AM (as distinct from sexual selection) depends on the context of divergence. Broadly speaking, assortment is likely to be important if diverged subgroups are present together at comparable frequencies, as in the center of a hybrid zone. Our theoretical approximations would not apply in this case, since F_1s would be sufficiently common as to mate among themselves and generate F_2 recombinants. Moreover, many hybrid zones are characterized by a bimodal distribution of parental ancestries or equivalently, of hybrid indices (Bridle and Butlin, 2002; Jiggins and Mallet, 2000; Schumer et al., 2017). The effects of AM in such a scenario are not amenable to simple descriptions which assume trait variance to increase by a constant factor $(1+\rho)/2$ (e.g., as in Muralidhar et al., 2022), since the correlation ρ between mating pairs in an assortatively mating population also depends on the distribution of phenotypic values and can be very different for unimodal versus bimodal populations. The consequences of nonrandom mating in hybrid zones thus remain an important direction for future work (see also Irwin, 2020), which will require us to expand existing theoretical descriptions.

What are some limitations of our study? We have considered a model of AM via self-referencing, wherein individuals prefer mates with similar phenotypes. However, sexual selection may be less effective in suppressing gene flow if female preference and the male traits on which it acts are encoded by

different genes, requiring these to be in LD. More generally, little is known about the prevalence of different mechanisms of AM and the extent to which these generate sexual selection in different ecological contexts (Kopp et al., 2018; Safran et al., 2013), making it important to examine the robustness of theoretical findings to alternative assumptions about assortment mechanisms.

We also consider an extreme form of divergent ecological selection, where alternative alleles are favored in the two populations at every locus. In this case, sexual selection is predominantly directional, reducing the mating success of individuals in proportion to their migrant ancestry. Alternatively, the magic trait could be under stabilizing selection toward different optima in the two populations. While selection on migrants would still be directional if trait optima are far apart, adaptive divergence can now be maintained at higher migration rates (Sachdeva and Barton, 2017). This results in a more complicated interplay between assortment and sexual selection, since mating between individuals with recent migrant ancestry becomes more common. Importantly, in this case, we need to go beyond theory that treats introgressing alleles as cascading down successively fitter genetic backgrounds, explicitly account for F2s, etc.

Finally, we neglect linkage between trait loci, which generally strengthens barriers to gene flow, at least under ecological divergent selection (Barton and Bengtsson, 1986). However, if traits are under frequency-dependent sexual selection, then linkage between trait loci may have more subtle effects (Kirkpatrick and Nuismer, 2004), even weakening barriers to gene flow under some conditions (Aubier et al., 2024). Approximations based on effective migration rates should extend to loose linkage between trait loci (Zwaenepoel et al., 2024). However, the effects of tight linkage (e.g., between alleles clustered within supergenes or inversions) are more obscure.

We focus here on the interplay between natural and sexual selection at a *fixed* level of assortment and following secondary contact between diverged populations. Other questions remain as to how assortment evolves in the first place—e.g., when mating with conspecifics might be favored by selection, thus reinforcing divergence (Servedio and Noor (2003)). While our study does not address these questions, it does suggest that analyzing the evolution of assortment in terms of the RV (or effective rate of exchange) of modifiers of mate choice could be a fruitful direction for future work. More generally, effective migration rates link a "phenotypic" view of RI (based on fitness components of hybrids) with a "genic" view (that conceptualizes RI as a process that reduces gene flow and increases divergence across the genome), making them a powerful way of understanding RI.

Supplementary material

Supplementary material is available online at *Evolution*.

Data availability

Mathematica notebook for numerical analysis and deterministic simulations and Fortran code for individual-based simulations are available at https://doi.org/10.15479/AT:ISTA:17344.

Author contributions

P.S. and H.S. designed the study, did the mathematical analysis and simulations, and wrote the manuscript.

Conflict of Interest

The authors declare no conflict of interest.

Acknowledgments

We thank Nick Barton for useful comments on the manuscript. This research was supported by the Scientific Service Units (SSU) of Institute of Science and Technology Austria (ISTA) through resources provided by Scientific Computing (SciComp).

References

Aubier, T. G., Kopp, M., Linn, I. J., Puebla, O., Rafajlović M., & Servedio, M. R. (2024). Negative coupling: The coincidence of premating isolating barriers can reduce reproductive isolation. *Cold Spring Harbor Perspectives in Biology*, *16*(10):a041435.

Barton, N. (1992). On the spread of new gene combinations in the third phase of Wright's shifting-balance. *Evolution*, *46*(2):551–557.

Barton, N., & Bengtsson, B. O. (1986). The barrier to genetic exchange between hybridising populations. *Heredity*, *57*(3):357–376.

Barton, N. H. (1983). Multilocus clines. *Evolution*, *37*(3):454–471.

Barton, N. H., & De Cara, M. A. R. (2009). The evolution of strong reproductive isolation. *Evolution*, *63*(5):1171–1190.

Barton, N. H., & Etheridge, A. M. (2011). The relation between reproductive value and genetic contribution. *Genetics*, *188*(4):953–973.

Barton, N. H., Etheridge, A. M., & Véber, A. (2017). The infinitesimal model: Definition, derivation, and implications. *Theoretical Population Biology*, *118*:50–73.

Bengtsson, B. (1985). The flow of genes through a genetic barrier. In *Evolution: Essays in honour of John Maynard Smith*, (pp. 31–42). Cambridge University Press.

Bridle, J. R., & Butlin, R. K. (2002). Mating signal variation and bimodality in a mosaic hybrid zone between *Chorthippus* grasshopper species. *Evolution*, *56*(6):1184–1198.

Butlin, R. K., & Smadja, C. M. (2018). Coupling, reinforcement, and speciation. *American Naturalist*, *191*(2):155–172.

Bérénos, C., Ellis, P. A., Pilkington, J. G., & Pemberton, J. M. (2014). Estimating quantitative genetic parameters in wild populations: A comparison of pedigree and genomic approaches. *Molecular Ecology*, *23*(14):3434–3451.

Chen, N., Juric, I., Cosgrove, E. J., Bowman, R., Fitzpatrick, J. W., Schoech, S. J., Clark, A. G., & Coop, G. (2019). Allele frequency dynamics in a pedigreed natural population. *Proceedings of the National Academy of Sciences*, *116*(6):2158–2164.

Coughlan, J. M., & Matute, D. R. (2020). The importance of intrinsic postzygotic barriers throughout the speciation process. *Philosophical Transactions of the Royal Society B: Biological Sciences*, *375*(1806):20190533.

Coyne, J. A., & Allen Orr, H. (2004). *Speciation*. Sinauer Associates.

Crow, J. F., & Felsenstein, J. (1968). The effect of assortative mating on the genetic composition of a population. *Eugenics Quarterly*, *15*(2):85–97.

Doebeli, M. (1996). A quantitative genetic competition model for sympatric speciation. *Journal of Evolutionary Biology*, *9*(6):893–909.

Elmer, K. R., Lehtonen, T. K., & Meyer, A. (2009). Color assortative mating contributes to sympatric divergence of neotropical cichlid fish. *Evolution*, *63*(10):2750–2757.

Felsenstein, J. (1981). Skepticism towards Santa Rosalia, or why are there so few kinds of animals? *Evolution*, *35*(1):124–138.

Fisher, R. A. (1918). The correlation between relatives on the supposition of mendelian inheritance. *Proceedings of the Royal Society of Edinburgh*, *52*:399–433.

Fisher, R. A. (1999). *The genetical theory of natural selection: A complete variorum edition*. Oxford University Press.

Fraïsse, C., & Sachdeva, H. (2021). The rates of introgression and barriers to genetic exchange between hybridizing species: Sex chromosomes *vs* autosomes. *Genetics*, *217*(2):iyaa025.

Irwin, D. E. (2020). Assortative mating in hybrid zones is remarkably ineffective in promoting speciation. *The American Naturalist*, *195*(6):E150–E167.

Jiang, Y., Bolnick, D. I., & Kirkpatrick, M. (2013). Assortative mating in animals. *The American Naturalist*, *181*(6):E125–138.

Jiggins, C. D., & Mallet, J. (2000). Bimodal hybrid zones and speciation. *Trends in Ecology & Evolution*, *15*(6):250–255.

Jiggins, C. D., Naisbit, R. E., Coe, R. L., & Mallet, J. (2001). Reproductive isolation caused by colour pattern mimicry. *Nature*, *411*(6835):302–305.

Johannesson, K., Havenhand, J. N., Jonsson, P. R., Lindegarth, M., Sundin, A., & Hollander, J. (2008). Male discrimination of female mucous trails permits assortative mating in a marine snail species. *Evolution*, *62*(12):3178–3184.

Kirkpatrick, M. (2000). Reinforcement and divergence under assortative mating. *Proceedings of the Royal Society of London. Series B: Biological Sciences*, *267*(1453):1649–1655.

Kirkpatrick, M., & Nuismer, S. L. (2004). Sexual selection can constrain sympatric speciation. *Proceedings of the Royal Society of London. Series B: Biological Sciences*, *271*(1540):687–693.

Kirkpatrick, M., & Ravigné, V. (2002). Speciation by natural and sexual selection: Models and experiments. *The American Naturalist*, *159*(S3):S22–S35.

Kobayashi, Y., Hammerstein, P., & Telschow, A. (2008). The neutral effective migration rate in a mainland-island context. *Theoretical Population Biology*, *74*(1):84–92.

Kondrashov, A. S., & Shpak, M. (1998). On the origin of species by means of assortative mating. *Proceedings of the Royal Society of London. Series B: Biological Sciences*, *265*(1412):2273–2278.

Kopp, M., Servedio, M. R., Mendelson, T. C., Safran, R. J., Rodríguez, R. L., Hauber, M. E., Scordato, E. C., Symes, L. B., Balakrishnan, C. N., Zonana, D. M., & van Doorn, G. S. (2018). Mechanisms of assortative mating in speciation with gene flow: Connecting theory and empirical research. *The American Naturalist*, *191*(1):1–20.

Lewontin, R., Kirk, D., & Crow, J. (1968). Selective mating, assortative mating, and inbreeding: Definitions and implications. *Eugenics Quarterly*, *15*(2):141–143.

Lynch, M., & Walsh, B. (1998). *Genetics and analysis of quantitative traits* (vol. 1). Sinauer Sunderland.

Maan, M. E., & Seehausen, O. (2011). Ecology, sexual selection and speciation. *Ecology Letters*, *14*(6):591–602.

Magurran, A. E., & Ramnarine, I. W. (2004). Learned mate recognition and reproductive isolation in guppies. *Animal Behaviour*, *67*(6):1077–1082.

Merrill, R. M., Wallbank, R. W. R., Bull, V., Salazar, P. C. A., Mallet, J., Stevens, M., & Jiggins, C. D. (2012). Disruptive ecological selection on a mating cue. *Proceedings of the Royal Society B: Biological Sciences*, *279*(1749):4907–4913.

Muralidhar, P., Coop, G., and Veller, C. (2022). Assortative mating enhances postzygotic barriers to gene flow via ancestry bundling. *Proceedings of the National Academy of Sciences*, *119*(30):e2122179119.

Nosil, P., Feder, J. L., Flaxman, S. M., & Gompert, Z. (2017). Tipping points in the dynamics of speciation. *Nature Ecology & Evolution*, *1*(2):0001.

Perini, S., Rafajlović, M., Westram, A. M., Johannesson, K., & Butlin, R. K. (2020). Assortative mating, sexual selection, and their consequences for gene flow in *Littorina*. *Evolution*, *74*(7):1482–1497.

Polechová, J., & Barton, N. H. (2005). Speciation through competition: A critical review. *Evolution*, *59*(6):1194–1210.

Ramsey, J., Bradshaw Jr, H., & Schemske, D. W. (2003). Components of reproductive isolation between the monkeyflowers *Mimulus lewisii* and *M. cardinalis* (phrymaceae). *Evolution*, *57*(7):1520–1534.

Rice, W. R., & Hostert, E. E. (1993). Laboratory experiments on speciation: what have we learned in 40 years? *Evolution*, *47*(6):1637–1653.

Rosenthal, G. G. (2013). Individual mating decisions and hybridization. *Journal of Evolutionary Biology*, *26*(2):252–255.

Rundle, H. D., & Nosil, P. (2005). Ecological speciation. *Ecology Letters*, *8*(3):336–352.

Sachdeva, H. (2022). Reproductive isolation via polygenic local adaptation in sub-divided populations: Effect of linkage disequilibria and drift. *PLOS Genetics*, *18*(9):e1010297.

Sachdeva, H., & Barton, N. H. (2017). Divergence and evolution of assortative mating in a polygenic trait model of speciation with gene flow. *Evolution*, *71*(6):1478–1493.

Safran, R. J., Scordato, E. S., Symes, L. B., Rodríguez, R. L., & Mendelson, T. C. (2013). Contributions of natural and sexual selection to the evolution of premating reproductive isolation: A research agenda. *Trends in Ecology & Evolution*, *28*(11):643–650.

Schumer, M., Powell, D. L., Delclós, P. J., Squire, M., Cui, R., Andolfatto, P., & Rosenthal, G. G. (2017). Assortative mating and persistent reproductive isolation in hybrids. *Proceedings of the National Academy of Sciences*, *114*(41):10936–10941.

Servedio, M. R. (2009). The role of linkage disequilibrium in the evolution of premating isolation. *Heredity*, *102*(1):51–56.

Servedio, M. R. (2016). Geography, assortative mating, and the effects of sexual selection on speciation with gene flow. *Evolutionary Applications*, *9*(1):91–102.

Servedio, M. R., & Boughman, J. W. (2017). The role of sexual selection in local adaptation and speciation. *Annual Review of Ecology, Evolution, and Systematics*, *48*(1):85–109.

Servedio, M. R., & Bürger, R. (2014). The counterintuitive role of sexual selection in species maintenance and speciation. *Proceedings of the National Academy of Sciences*, *111*(22):8113–8118.

Servedio, M. R., Doorn, G. S. V., Kopp, M., Frame, A. M., & Nosil, P. (2011a). Magic traits in speciation: 'magic' but not rare? *Trends in Ecology & Evolution*, *26*(8):389–397.

Servedio, M. R., Doorn, G. S. V., Kopp, M., Frame, A. M., & Nosil, P. (2011b). Magic traits in speciation: 'magic' but not rare? *Trends in Ecology & Evolution*, *26*(8):389–397.

Servedio, M. R., & Kopp, M. (2012). Sexual selection and magic traits in speciation with gene flow. *Current Zoology*, *58*(3):510–516.

Servedio, M. R., & Noor, M. A. (2003). The role of reinforcement in speciation: Theory and data. *Annual Review of Ecology, Evolution, and Systematics*, *34*(1):339–364.

Smadja, C. M. and Butlin, R. K. (2011). A framework for comparing processes of speciation in the presence of gene flow. *Molecular Ecology*, *20*(24):5123–5140.

Smith, J. M. (1966). Sympatric Speciation. *The American Naturalist*, *100*(916):637–650.

Sobel, J. M., & Chen, G. F. (2014). Unification of methods for estimating the strength of reproductive isolation. *Evolution*, *68*(5):1511–1522.

Stelkens, R. B., & Seehausen, O. (2009). Phenotypic divergence but not genetic distance predicts assortative mating among species of a cichlid fish radiation. *Journal of Evolutionary Biology*, *22*(8):1679–1694.

Vines, T. H., & Schluter, D. (2006). Strong assortative mating between allopatric sticklebacks as a by-product of adaptation to different environments. *Proceedings of the Royal Society B: Biological Sciences*, *273*(1589):911–916.

Westram, A. M., Stankowski, S., Surendranadh, P., & Barton, N. (2022). What is reproductive isolation? *Journal of Evolutionary Biology*, *35*(9):1143–1164.

Wright, S. (1921). Systems of Mating. III. Assortative mating based on somatic resemblance. *Genetics*, *6*(2):144–161.

Wright, S. (1937). The distribution of gene frequencies in populations. *Proceedings of the National Academy of Sciences*, *23*(6):307–320.

Zwaenepoel, A., Sachdeva, H., & Fraïsse, C. (2024). The genetic architecture of polygenic local adaptation and its role in shaping barriers to gene flow. *Genetics*, *228*(3):iyae140.